Phenotypic Variation in Enhanced S-cone Syndrome

Isabelle Audo,[1,2,3,4] *Michel Michaelides,*[1,2,4] *Anthony G. Robson,*[1,2] *Marko Hawlina,*[5] *Veronika Vaclavik,*[1,2] *Jennifer M. Sandbach,*[1,6] *Magella M. Neveu,*[1] *Chris R. Hogg,*[1] *David M. Hunt,*[2] *Anthony T. Moore,*[1,2] *Alan C. Bird,*[1,2] *Andrew R. Webster,*[1,2] *and Graham E. Holder*[1,2]

Purpose. To characterize the clinical, psychophysical, and electrophysiological phenotype of 19 patients with enhanced S-cone syndrome (ESCS) and relate the phenotype to the underlying genetic mutation.

Methods. Patients underwent ophthalmic examination and functional testing including pattern ERG, full-field ERG, and long-duration and short-wavelength stimulation. Further tests were performed in some patients, including color contrast sensitivity (CCS), multifocal ERG, fundus autofluorescence imaging (FAI), optical coherence tomography (OCT), and fundus fluorescein angiography (FFA). Mutational screening of *NR2E3* was undertaken in 13 patients.

Results. The fundus appearance was variable, from normal to typical nummular pigment clumping at the level of the retinal pigment epithelium in older patients. Nine patients had foveal schisis, and one had peripheral schisis. Pattern ERG was abnormal in all patients. In all patients, ISCEV Standard photopic and scotopic responses had a similar waveform, the rod-specific-ERG was undetectable and the 30-Hz flicker ERG was markedly delayed with an amplitude lower than the photopic a-wave. Most ERG responses arose from short-wavelength–sensitive mechanisms, and a majority of patients showed possible OFF-related activity. Multifocal ERG showed relative preservation of central function, but reduced responses with increased eccentricity. Mutations were identified in *NR2E3* in 12 of 13 patients including four novel variants.

Conclusions. The phenotype in ESCS is variable, both in fundus appearance and in the severity of the electrophysiological abnormalities. The ERGs are dominated by short-wavelength–sensitive mechanisms. The presence, in most of the patients, of possible OFF-related ERG activity is a finding not usually associated with S-cones. (*Invest Ophthalmol Vis Sci.* 2008;49: 2082–2093) DOI:10.1167/iovs.05-1629

Enhanced S-cone syndrome (ESCS; OMIM 268100; http://www.ncbi.nlm.nih.gov/omim/ Online Mendelian Inheritance in Man; NCBI, Bethesda, MD) is a rare, slowly progressive autosomal recessive retinal degeneration related to mutation in *NR2E3*. Patients usually present with night blindness, variable loss of visual acuity and visual field abnormalities. There may be various fundus appearances, the most typical being nummular pigmentary deposition at the level of the retinal pigment epithelium (RPE), primarily along the vascular arcades, and macular disturbance, often associated with intraretinal cysts.[1,2] There are pathognomonic electroretinographic features: photopic and scotopic responses to the same stimulus have a similar waveform and have been shown to be dominated by short-wavelength–sensitive mechanisms.[1–4] Short-wavelength–specific responses are of higher amplitude than those of normal subjects. The pathognomonic nature of the ERG changes allows the diagnosis to be established by standard ERG recording. The use of additional short-wavelength–specific stimulation is not necessary for diagnosis, but can provide valuable adjunctive information to aid our understanding of the underlying mechanisms.

Histopathologic data have been reported from one elderly patient with advanced disease.[5] There was an absence of rods, but a two-fold increase in the cone population, most of which were thought to be S-cones. Fifteen percent of the cones expressed L/M-cone opsin including some which co-expressed S-cone opsin. The retina was highly degenerated and disorganized. Photoreceptors were found only in the central and far peripheral regions. Densely packed cones were intermixed with inner retinal neurons. The increased number of cones in ESCS is unique, since, as a group of disorders, the progressive retinal dystrophies are usually characterized by a loss of photoreceptors.

Mutations in the *NR2E3* gene (also known as photoreceptor-specific nuclear receptor (PNR; OMIM 604485) have been found in both ESCS and Goldman-Favre Syndrome (GFS).[6–8] A naturally occurring recessive *NR2E3* mutation has also been identified in the *rd7* mouse and has helped further to probe the disease process.[9–12]

NR2E3 encodes a ligand-dependent transcription factor that controls retinal progenitor cell fate.[13,14] It promotes differentiation and survival of rod photoreceptors by differentially regulating transcription of rod- and cone-specific genes either directly or indirectly through interaction with other transcription factors, including CRX and NRL.[14–17] Mutation in *NR2E3* is thought to cause disordered photoreceptor cell differentiation, possibly by encouraging default from the rod photoreceptor pathway to the S-cone pathway, thereby altering the relative ratio of cone subtypes.[5,14,18,19] However, to date, *NR2E3* expression has been identified only in rod photoreceptors.[6,10,13,15,16]

The purpose of the present study was to review the detailed phenotype of a panel of patients with a diagnosis of ESCS and

From [1]Moorfields Eye Hospital, London, United Kingdom; [2]Institute of Ophthalmology, University College London, London, United Kingdom; [3]Laboratoire de Physiopathologie Cellulaire Moléculaire et de la Rétine, Inserm U592, Université Pierre et Marie Curie, Paris, France; the [5]University Eye Hospital, Medical Centre Ljubljana, Ljubljana, Slovenia; and the [6]Department of Ophthalmology, Prince of Wales Hospital, Randwick, NSW, Australia.

[4]Contributed equally to the work and therefore should be considered equivalent authors.

Supported by EVI-Genoret FP6 Integrated Project LSHG-CT-2005-512036, British RP Society, and a Career Development Award from Foundation Fighting Blindness (IA).

Submitted for publication December 20, 2005; revised June 30, 2006, and March 5, 2007; accepted March 25, 2008.

Disclosure: **I. Audo**, None; **M. Michaelides**, None; **A.G. Robson**, None; **M. Hawlina**, None; **V. Vaclavik**, None; **J.M. Sandbach**, None; **M.M. Neveu**, None; **C.R. Hogg**, None; **D.M. Hunt**, None; **A.T. Moore**, None; **A.C. Bird**, None; **A.R. Webster**, None; **G.E. Holder**, None

The publication costs of this article were defrayed in part by page charge payment. This article must therefore be marked "*advertisement*" in accordance with 18 U.S.C. §1734 solely to indicate this fact.

Corresponding author: Graham E. Holder, Department of Electrophysiology, Moorfields Eye Hospital, 162 City Road, London EC1V 2PD, UK; graham.holder@moorfields.nhs.uk.

TABLE 1. Primers Used for NR2E3 Amplification and the Corresponding Annealing Temperatures

Primer	Sequence (5′–3′)	Annealing Temp./Time
Exon 1 F	acaggggcacagagagacag	
Exon 1 R	aacctctggcccttaccct	60 for 1 min
Exons 2 & 3 F	tccagatggaagagtcacg	
Exons 2 & 3 R	tcaggacgacacgccagt	56 for 30 s
Exon 4 F	actggcgtgtcgtcctga	
Exon 4 R	gaagccaagccctgctgt	54 for 30 s
Exon 5 F	caagtactccctgccacctc	
Exon 5 R	gtaggtacctgatcccggaag	56 for 30 s
Exon 6 F	tgagccagagaagctgtgtg	
Exon 6 R	ctggcttgaagaggaccaag	55 for 30 s
Exon 7 F	ggcgtggagtgaactctttc	
Exon 7 R	ggagagtgagaggcagatgg	55 for 30 s
Exon 8 F	ctgtgctaagctcgactggtg	
Exon 8 R	gaggtcagggacaaatgagtg	60 for 30 s
Exon 9 F	gtcgtaaaactgatggcgtcctc	
Exon 9 R	gcaaatgtttcgtttcagtagattg	60 for 30 s

subsequently to characterize the proportion and nature of *NR2E3* mutations in this cohort.

METHODS

Nineteen patients, 13 simplex cases, 2 sibling pairs (2 brothers and 2 sisters), and 1 father and daughter with ESCS were ascertained. The protocol of the study adhered to the tenets of the Declaration of Helsinki and was approved by the local Ethics Committee.

Each patient underwent full ophthalmic examination after providing informed consent. Full-field and pattern electroretinography (ERG and PERG) were performed with gold foil recording electrodes (HK-loop electrodes in patients 15 and 16) and incorporated the ISCEV Standards.[20,21] A stimulus 0.6 log units stronger than the ISCEV standard flash was used to elicit the bright flash ERG, the better to demonstrate the dark-adapted a-wave.[21] A light-emitting diode–based mini-Ganzfeld was used to elicit S-cone ERGs[22] and ON and OFF responses. S-cone ERGs used a blue stimulus (445 nm, 80 cd/m^2) on an orange background (620 nm, 560 cd/m^2), with the same orange stimulus of 200-ms duration used with a green background (530 nm, 160 cd/m^2) for ON and OFF responses from the L/M-cone systems. Stimulus duration for the blue stimulus was varied from 1 to 10 ms for short-duration flashes, and was 200 ms for the long-duration flashes used to examine ON and OFF responses. Further tests were performed in some patients including color contrast sensitivity (CCS, 9/19 patients), multifocal ERG (6/19), fundus autofluorescence imaging (FAI, 7/19), optical coherence tomography (OCT, 4/19) and fundus fluorescein angiography (FFA, 5/19). CCS was assessed according to previously described techniques.[23,24]

NR2E3 was screened for disease-causing mutations in all patients who consented to give blood samples (n = 13). Total genomic DNA was extracted from peripheral blood leukocytes (Nucleon II Biosciences kit; Scotlab Ltd., Strathclyde, UK). The gene *NR2E3* is located on chromosome 15, arm q23, and has nine exons encoding a protein of 409 residues. Coding sequences and splice-junction sites of *NR2E3* were amplified by polymerase chain reaction (PCR) in each individual by using the primer sequences and annealing temperatures shown in Table 1. PCR reactions (50 μL) were performed as follows: 1 × NH_4 reaction buffer (Bioline, London, UK), 1 mM $MgCl_2$, 200 μM each dNTP, 10 picomoles each of forward and reverse primers, 200 ng to 1 μg DNA, and1 U *Taq* polymerase (Bio*Taq*; Bioline). After resolution on a 1% (wt/vol) low-melting-temperature agarose gel, the products were excised and eluted. Direct sequencing of PCR products was performed on a genetic analyser (model 3100; Applied Biosystems [ABI], Warrington, UK) using the original PCR primers in the sequencing reactions. The sequence was examined for alterations using sequencing analysis (Prism with GeneWorks software; ABI). GenBank sequences were used to construct an alignment of nuclear receptor sequences to analyze the evolutionary conservation of the corresponding amino acid positions. Sequences were aligned with the software (GeneWorks software; ABI).

RESULTS

Clinical Evaluation

The 19 patients included in this series were of diverse ethnic and geographical origin, including Pakistan, Iran, The Philippines, and Europe. A clear history of consanguinity was present in two cases. The clinical findings are summarized in Table 2.

The clinical presentation in all patients was night blindness, with or without reduced central vision. Nyctalopia had begun in early childhood with onset ranging from 2 to 6 years of age. No patient reported photophobia. Visual acuity ranged between 6/6 and 3/60. A hypermetropic refractive error with a variable degree of astigmatism was identified in most of the patients for whom data were available. Five patients described worsening of their symptoms. In one, there was a documented reduction in visual acuity from 6/6 to 6/24 over a 20-year period. Nystagmus was not present in any patient.

Vitreous cells were present in all patients. Two subjects exhibited more prominent vitreous changes including vitreous opacities, haze, and veils. The fundus appearance varied extensively between patients (Fig. 1). The youngest subject had normal appearing fundi. Six patients had subtle to mild pigmentary changes with focal hyperpigmentation (Figs. 1a–c), with one of these subjects having small yellow-white dots at the posterior pole. The most distinctive ophthalmoscopic feature was nummular pigmentary deposition at the level of the RPE, usually located in the mid periphery along the vascular arcades and often associated with RPE atrophy (Figs. 1a, 1d–f). This characteristic pigmentary clumping was noted in 12 of 19 patients. In addition, yellow-white deposits were also present in areas of marked pigmentary abnormalities or within the posterior pole (Fig. 1d). Foveal schisis-like changes were observed in nine patients. OCT was performed in four of those patients and demonstrated foveal cyst formation (Fig. 1b). Cystoid macular edema was originally diagnosed on clinical examination in three of nine patients. Oral acetazolamide therapy produced no documented improvement. Subsequently, these patients had FFA, which showed no leakage (Fig. 2), suggesting that the cystoid changes were more likely to be secondary to schisis than to edema. One patient had peripheral schisis (Fig. 1d).

FAI showed four distinctive types of abnormality. There was a decrease or lack of autofluorescence (AF) outside the arcades in severely affected cases (Figs. 1a, 1e, 2a). Some patients showed a ring of relatively increased AF in the transitional zone between this area of decreased/absent AF and the macular region (Fig. 1e). The small hyperpigmented areas within the arcades were associated with a focal increase of AF (Figs. 1b, 1c). Patients with foveal schisis had a spoke-like area of relatively increased AF centered on the fovea (Figs. 1b, 2a).

Functional Evaluation

The functional findings are summarized in Table 3 Color contrast sensitivity (CCS) was tested in nine patients. Two had normal color vision. In one, a generalized dyschromatopsia was revealed, whereas six of nine patients demonstrated relative tritan axis sparing and moderately elevated protan and deutan thresholds.

The pattern ERG, when detectable, was usually markedly delayed. The P50 component was of normal amplitude but delayed in three patients and delayed and reduced in 11 patients, and the PERG was undetectable in five patients.

TABLE 2. Summary of Clinical Findings in ESCS

Patient	Sex	Age	VA	Refraction	Other Findings	Fundus
1	F	12	OD: 6/9 OS: 6/12	+3.5/+1.25 × 90 +6.5/+1.50 × 90	Left convergent squint Left amblyopia	Schisis-like macular appearance Subtle pigmentary changes with small hyperpigmented areas within the vascular arcades
2	M	16	OD: 6/6 OS: 6/6	Low hyperopic astigmatism	—	Subtle pigmentary changes with small hyperpigmented areas within the vascular arcades (Fig. 1c)
3	M	43	OD: 6/9 OS: 6/9	+2.0/+0.75 × 90 +1.0/+2.0 × 30	—	Mid-peripheral nummular pigment clumping and atrophy at level of RPE
4	F	19	OD: 6/9 OS: 6/9	Low myopia	Vitreous changes	Subtle mid-peripheral nummular pigment clumping at level of RPE (Fig. 1a)
5	F	20	OD: 6/12 OS: 6/18	+4.75/−0.75 × 175 +4.75/−0.75 × 10	Left convergent squint Left amblyopia	Peripheral retinoschisis Mid-peripheral nummular pigment clumping and atrophy at level of RPE (Fig. 1d)
6	F	32	OD: 6/24 OS: 6/24	+4.0/+0.50 × 180 +5.0 DS	Vitreous changes	Mid-peripheral nummular pigment clumping and atrophy at level of RPE
7	F	41	OD: 6/12 OS: 6/36	Hypermetropia	Constricted visual fields	Mid-peripheral nummular pigment clumping and atrophy at level of RPE
8	F	42	OD: 3/60 OS: 6/36	Hypermetropia	Right convergent squint with amblyopia Constricted visual fields	Mid-peripheral nummular pigment clumping and atrophy at level of RPE
9	M	33	OD: 3/60 OS: 3/60	ND	—	Macular schisis Mid-peripheral nummular pigment clumping and atrophy at level of RPE
10	F	6	OD: 6/9 OS: 6/9	+2.50/−1.25 × 180 +2.25/−1.25 × 180	Convergent squint	Normal fundus
11	M	35	OD: 6/60 OS: 6/36	+4.50/−0.50 × 145 +0.50/−1.0 × 140	Constricted visual fields	Macular cysts documented by OCT Mid-peripheral nummular pigment clumping and atrophy at level of RPE
12	F	72	OD: 6/9 OS: 6/12	ND	Constricted visual fields	White dots and subtle mid-peripheral pigmentary changes
13	M	20	OD: 6/60 OS: 6/60	+5.50/−1.75 × 25 +4.75/−1.50 × 160	—	Macular cysts documented by OCT Subtle mid-peripheral pigmentary changes at level of RPE
14	M	25	OD: 6/18 OS: 6/36	Hypermetropia	—	Macular cysts documented by OCT Subtle pigmentary changes with small hyperpigmented areas within the vascular arcades (Fig. 1b)
15	M	24	OD: 6/36 OS: 6/12	+1.00/−1.00 × 180 +2.00/−1.50 × 170	Constricted visual field, relative central scotoma Left convergent squint	Asymmetrical macular cysts documented by RTA with no leakage on FFA Mid-peripheral nummular pigment clumping and atrophy at level of RPE
16	M	26	OD: 6/18 OS: 6/36	+1.00/−1.00 × 180 +2.00/−1.50 × 170	Constricted visual field, relative central scotoma	Symmetrical macular cysts (Fig. 1f) documented by RTA with no leakage on FFA Mid-peripheral nummular pigment clumping and atrophy at level of RPE (Fig. 2)
17	M	48	OD: 6/18 OS: 6/18	ND	—	Mid-peripheral nummular pigment clumping and atrophy at level of RPE (Fig. 1e)
18	M	32	OD: 6/9 OS: 6/9	ND	Constricted visual fields	Left macular cysts Mid-peripheral nummular pigment clumping and atrophy at level of RPE
19	F	25	OD: 6/12 OS: 6/12	−1.75/−2.00 × 10 −1.75/−1.50 × 10	—	Macular cysts documented by OCT Subtle mid-peripheral pigmentary changes

Patients 7 and 8 are sisters, 9 and 10 are father and daughter; 15 and 16 are brothers; ND: not documented; RTA: Retinal Thickness Analyzer (Talia Technologies, Israel).

All patients had pathognomonic ERG waveforms (Figs. 3, 4). The rod-specific ERG was undetectable; the ERG response to a standard single flash had similar waveforms under photopic and scotopic conditions; and the 30-Hz flicker ERG was both delayed and of lower amplitude than the single-flash photopic ERG a-wave. Such findings establish the diagnosis with or without the use of specific short-wavelength stimulation. Included in Table 3 is an evaluation of each patient based on the dark-adapted bright flash a-wave as a percentage of the lower limit of normal (the absolute normal values differ between the two units from which the patients have been ascertained). However, it is stressed that the scotopic a-wave in ESCS is likely to be arising from dark-adapted short-wavelength–sensitive cones (as opposed to the rod-dominated a-wave in a normal retina), is also of markedly longer peak time, and the use of this measure is not intended to imply physiological equivalence, merely to allow an estimate of the overall severity of the disorder in each patient. ERG amplitudes showed high variability between patients related to the severity of degeneration, with older patients tending to have the more severe abnormalities.

Specific chromatic stimulation was studied in most patients and showed that most of the ERG responses were arising from short-wavelength–sensitive systems with abnormally large S-cone ERGs (relative to those with standard stimulation) and

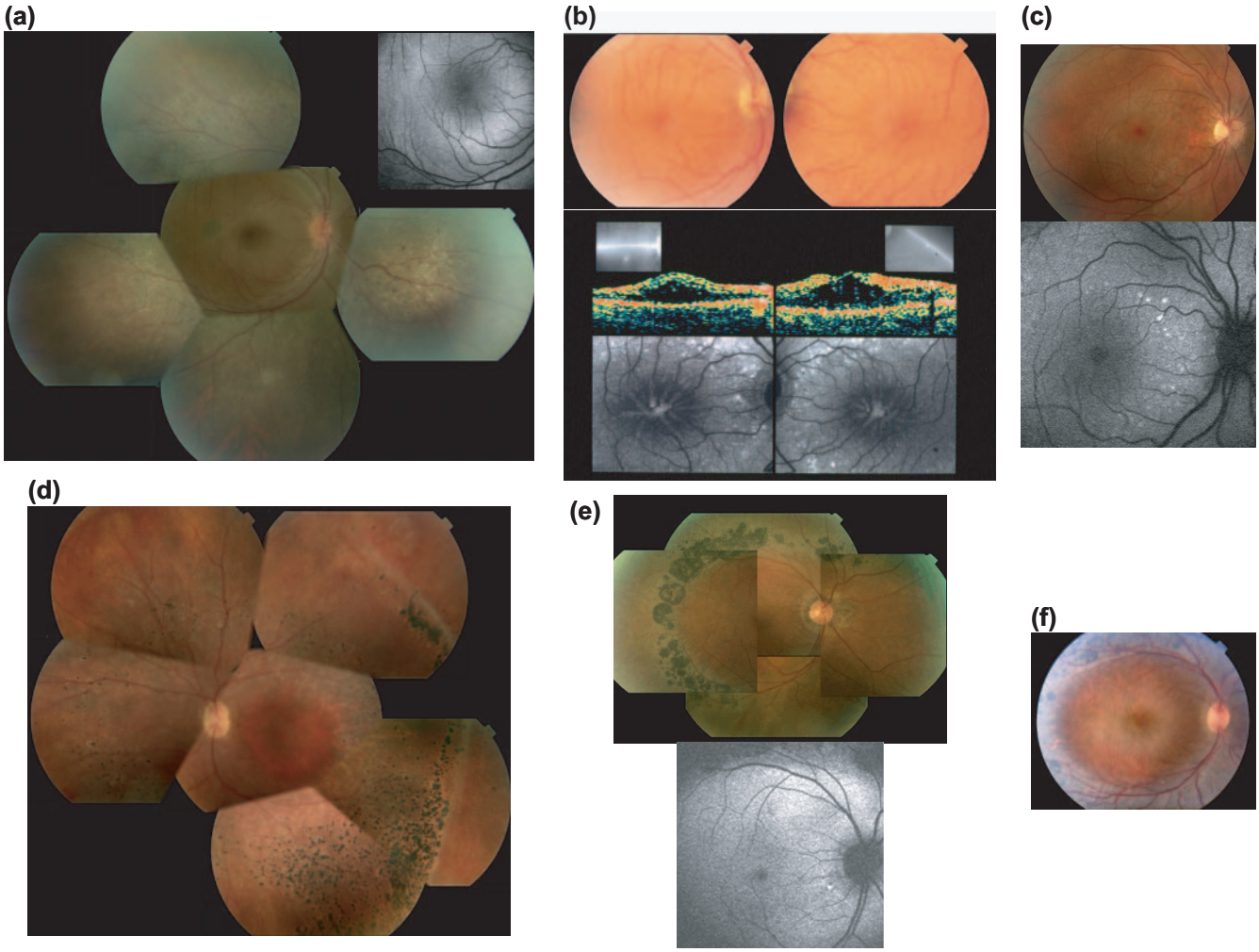

FIGURE 1. Variability of the clinical phenotype. (**a**) Patient 4, subtle pigmentary changes along the vascular arcades, with an absence of AF outside the arcades; (**b**) patient 14, macular disturbance with subtle pigmentary changes and areas of hyperpigmentation within the vascular arcades associated with increased AF on FAI. Foveal schisis is demonstrated on OCT; (**c**) patient 2, areas of hyperpigmentation within the vascular arcades associated with increased AF on FAI; (**d**) patient 5, nummular pigmentary deposits at the level of the RPE with peripheral schisis present; (**e**) patient 17, nummular pigmentary clumping at the level of the RPE along the vascular arcades. There is a ring of increased AF at the posterior pole on FAI but no AF detectable outside the arcades; (**f**) patient 16, nummular pigmentary deposition at the level of the RPE along the vascular arcades with macular schisis (see Fig 2).

minimal responses to L/M-cone stimulation. Representative examples showing ERG responses to a range of stimulus intensities appear in Figures 3b and 4b[b], from patients 2, 4, and 14, and even with 1-ms stimulus duration, there is a well-developed S-cone ERG, but of simplified waveform and increased latency. A prominent a-wave develops with increasing stimulus duration that could reach up to 100 μV with an implicit time of 28 ms in response to a 10-ms flash (Fig. 4b). When the blue stimulus duration was increased to 200 ms, the a-wave was relatively unchanged, suggesting that saturation of the a-wave was complete with the 10-ms stimulus. The b-wave, however, declined in amplitude, giving a "negative" ON-response waveform and thus raising the possibility that OFF- activity had contributed to the b-wave with the shorter duration stimulus. The responses to 10- and 200-ms blue stimulation (Fig. 5) indicate that most patients showed b-wave reduction with an increase in stimulus duration, and possible OFF activity, which, when present, consisted of a d-wave of amplitude similar to that of the b-wave but with a sustained plateau and a failure to return rapidly to baseline. An orange stimulus with a green background evoked only small or undetectable L/M-cone ERGs in all patients tested (data not shown).

An EOG light increase was undetectable in the eight patients in whom EOG was performed. Multifocal ERG was performed in 6 of 19 individuals and showed well formed responses to the central hexagons, but considerable reduction/absence of responses with increasing eccentricity (Fig. 3c). Multifocal ERGs were of simplified waveform and delayed. Only two patients had both mfERG and OCT. There was no obvious relationship between the two.

Visual field data have been described when available; these data are not available for all patients.

NR2E3 Mutation Screening

Screening of the nine coding exons of NR2E3 was performed in 13 of 19 patients. Mutations were identified in 12 of 13 subjects: with 8 subjects being homozygous, 3 having compound heterozygous mutations, and 1 heterozygous individual having no identified second mutation. Screening of *NR2E3* yielded eight sequence variants that most likely represent disease-causing mutations, including four novel mutations (Table 4). Four previously reported mutations were identified, a splice acceptor intron 1 mutation,[6–8] the Arg311Gln and Arg104Trp sub-

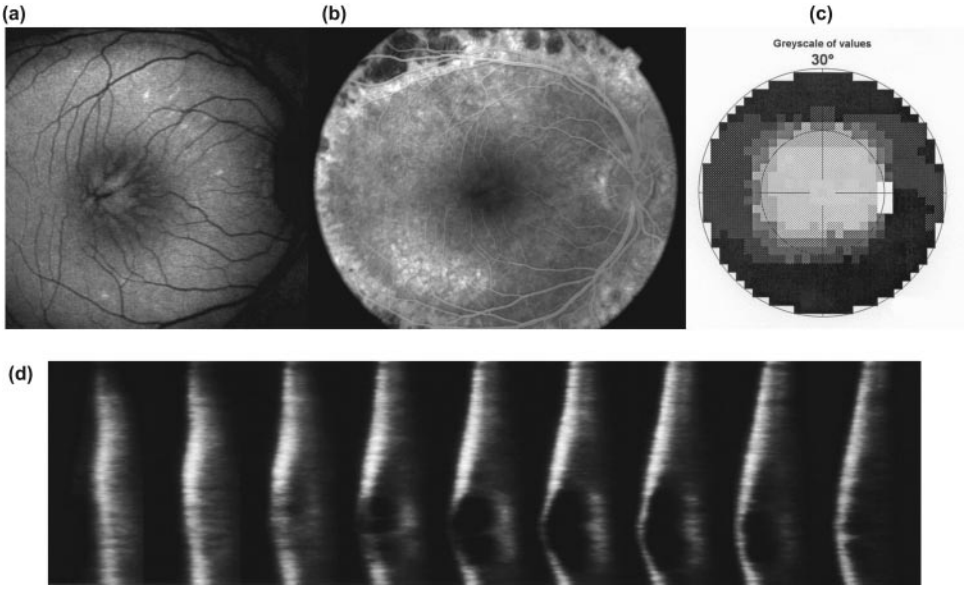

FIGURE 2. Cystic changes in a patient with ESCS. Patient 16: right-eye fundus autofluorescence (**a**), fluorescein angiography (**b**), and retinal thickness analyzer (**d**), documenting cystic changes. Central static perimetry of the right eye (**c**) shows peripheral loss of retinal sensitivity with relatively preserved central sensitivity despite schitic changes.

stitutions,[6–8] and the 481delA frameshift mutation.[8] The four novel mutations were two splice acceptor variants (introns 1 and 8) and two missense mutations (Val49Met and Tyr81Cys).

The previously reported splice acceptor intron 1 mutation (IVS1-2A>C) was identified as a heterozygous change in four patients and in the homozygous state in a single subject (Fig. 6a); the Arg311Gln (R311Q) substitution (932G→A; exon 6; ~45% of patients)[6] was found as a heterozygous change in patient 4 (Fig. 6b); the Arg104Trp (R104W) substitution (500C→T; exon 3) was identified as a homozygous change in patients 9 and 10 (father and daughter, respectively; the mother was found to be heterozygous for R104W, being a first cousin and unaffected); and the frameshift mutation, T161fs (481delA; exon 4), as a homozygous change in patients 15 and 16 (brothers; Fig. 6c). This frameshift mutation would generate a stop codon at position 178. The T161fs has been described only in the heterozygous state.[8] The R311Q mutation is far less prevalent in the sample in our study than in previous investigations.[6,8]

Two novel missense mutations were identified: the Val49Met (V49M) substitution (145G→A; exon 2; Fig. 6d) was identified as a homozygous change in patient 3; and the Tyr81Cys (Y81C) substitution (242A→G; exon 2; Fig. 6e) as a heterozygous change in patients 7 and 8 (sisters). Both Val49 and Tyr81 are conserved across other NR2E3 receptors, and neither missense mutation was found in a screen of 100 control chromosomes. V49M and Y81C are both located in the highly conserved DNA binding domain of NR2E3.

Two novel splice site mutations were identified: the first novel splice acceptor (3′ splice) mutation is a C→G nucleotide change at the intron 1 splice site (IVS1-3C>G) (Figs. 6f, 7), identified as a homozygous change in patient 13. One of the most common previously reported mutations in *NR2E3* is an A→C change at this same splice site.[6–8] A mutation identified in the present cohort in both heterozygous and homozygous states (5/10 patients). The second novel splice acceptor mutation identified is at intron 8 (IVS8-1G>A; Figs. 6g, 7), present as a homozygous change in patient 1. Neither novel splice acceptor mutation was found in a screen of 100 control chromosomes. The likely effect of the splice acceptor intron 1 and intron 8 mutations would be to cause aberrant splicing, resulting in either failure to remove these introns, or loss of exon 2 or 9, respectively, from the transcript as a result of splicing with the next intact splice acceptor site (Fig. 7). The loss of exon 9 would require splicing to an acceptor site downstream of the coding sequence of the gene. A retained intron may lead to premature termination of translation and a truncated protein that is either nonfunctional or has reduced efficacy. Loss of exons will result in the absence in the protein of amino acid residues encoded by these regions and since exons 2 and 9 encode residues involved in DNA-binding and ligand-binding, respectively, a transcription factor of significantly reduced function would be predicted. However, the loss of exon 2 would also generate a frameshift as intron 1 interrupts codon 40 of exons 1 and 2 at position 1, whereas intron 2 interrupts codon 82 of exons 2 and 3 at position 2, thus generating a stop codon in exon 3 and most likely resulting in nonsense-mediated mRNA decay in the aberrant transcript and the complete absence of any protein.

Two novel silent polymorphisms were demonstrated: A95A (285C→T; exon 3) and G288G (864T→A; exon 6).

DISCUSSION

A large cohort of patients with enhanced S-cone syndrome (ESCS) was ascertained from Moorfields Eye Hospital, with the contribution of two siblings (patients 15 and 16) by the University Eye Hospital, Ljubljana, Slovenia. The pathognomonic ERG changes previously reported by others are confirmed.[1–4,25,26] The variability of the phenotype is described, and novel data are presented in relation to pattern ERGs, multifocal ERGs, ON/OFF ERG responses, color contrast sensitivity and fundus autofluorescence imaging (FAI). Novel *NR2E3* mutations are described.

All subjects experienced nyctalopia at an early age. Visual acuity was variable from normal to severely reduced (3/60), but there was no correlation with age; some younger individuals had worse visual acuity than older patients. The presence of foveal schisis was often associated with poor visual acuity. The most common refractive error identified was hyperopia, with a variable degree of astigmatism, in keeping with previous reports.[2,7] Longitudinal ERG data were available for some patients and suggested slowly progressive dysfunction with gradual deterioration of visual acuity and variable visual field constriction. Color contrast sensitivity testing revealed sparing along the tritan axis in 6 of 9 patients. The findings also suggested some residual L- and M-cone–mediated function in keeping with the available histopathologic data.[5]

Fundus examination revealed a highly variable retinal phenotype, ranging from normal to marked pigmentary abnormal-

TABLE 3. Summary of Functional Findings in ESCS

Patient	CCS	PERG P50	Bright Flash DA a-Wave Amplitude (% Lower Limit of Normal) (RE/LE)	Large S-cone ERG	OFF Response	Other Findings
1	NP	Normal amplitude, delayed	81/84	Present	OFF response plateau	—
2	OD: 11/8/6.5 OS: NP	Delayed and mildly reduced	94/81	Present	Absent	Multifocal ERG: preserved responses to central hexagons but loss of the response to more peripheral hexagons
3	OD: 8/8.5/13.5 OS: 12.5/9.5/14	Delayed and reduced	6/6	NP	NP	—
4	OD: 6/6/7 OS: 7.5/6.5/6.5	Normal amplitude, delayed	50/46	Present	OFF response plateau	Multifocal ERG: preserved central responses but reduced with increasing eccentricity EOG light rise undetectable
5	OD: 6.5/6.5/5 OS: 6.5/6/4.5	Severely delayed and reduced	40/36	Present	OFF response plateau	Multifocal ERG: preserved central responses but reduced with increasing eccentricity
6	OD: 56/>100/8.5 OS: 78.5/>100/13.5	Not detectable	10/10	NP	NP	EOG light rise undetectable
7	OD: 24/27.5/8 OS: 32/40/8.5	Not detectable	10/10	Present	OFF response plateau	—
8	OD: NP OS: 38.5/48.5/10.5	Not detectable	27/27	Present	Absent	EOG light rise undetectable
9	NP	Not detectable	60/58	NP	NP	—
10	NP	Normal amplitude, delayed	61/73	Present	OFF response plateau	—
11	NP	Delayed and reduced	6/11	Small	Absent	—
12	NP	Delayed and reduced	21/21	Present	?	EOG light rise undetectable
13	NP	Not detectable	50/54	Present	?	EOG light rise undetectable
14	Sparing tritan axis	Delayed and reduced	90/96	Present	NP	
15	NP	Delayed and reduced	54/54	Present	NP	Multifocal ERG: preserved central responses but reduced with increasing eccentricity EOG light rise undetectable
16	NP	Delayed and reduced	61/47	Present	NP	Multifocal ERG: preserved central responses but reduced with increasing eccentricity EOG light rise undetectable
17	OD: 32.9/44.6/7.9 OS: 28.9/44.1/8.2	Delayed and reduced	31/42	Present	OFF response plateau	Multifocal ERG: responses absent, mostly background noise EOG light rise undetectable
18	NP	Reduced and delayed	23/24	Present	OFF response plateau	—
19	NP	Delayed and reduced	77/77	Present	Absent	—

Patients 7 and 8 are sisters; 9 and 10 are father and daughter; 15 and 16 are brothers. NP, not performed; CCS, color contrast sensitivity, for protan, deutan and tritan axis (normal values: <8/<8/<13) Bright flash dark adapted (DA) amplitude as a percentage of each laboratory lower limit of normal. The use of this measure is not intended to imply physiological equivalence, merely to allow an estimate of the overall severity of the disorder in each patient.

ities. The most typical ophthalmoscopic feature was the presence of nummular, mid-peripheral pigmentary deposits at the level of the RPE. This typical retinal appearance was associated with an absence of AF outside the vascular arcades on FAI, possibly relating to loss of photoreceptors in this region.[5] A ring of relatively increased AF in the transitional area between the region of absent AF and the central zone of relatively normal AF was evident. The increased AF detected may be related to lipofuscin accumulation secondary to RPE–photoreceptor dysfunction in that area.[27,28] Such rings have been described in the parafoveal region in both RP and cone–rod dystrophy (Robson AG, et al. *IOVS* 2005;46:ARVO E-Abstract 552).[29–35] Foveal schisis documented by FFA, OCT, or RTA was present in nine patients, in keeping with previous findings.[2]

The typical nummular, mid-peripheral pigmentary changes are a useful clinical sign, but are not a consistent finding, being evident in 12 of 19 patients in the present series. Sharon et al.[7] suggested that subtle pigmentary changes with white dots represent an early stage of the disease process, which progresses to the typical clumped retinopathy in later adulthood. The observation in the present cohort of a 72-year-old patient with only very subtle pigmentary changes does not support this suggestion and emphasizes the variability of fun-

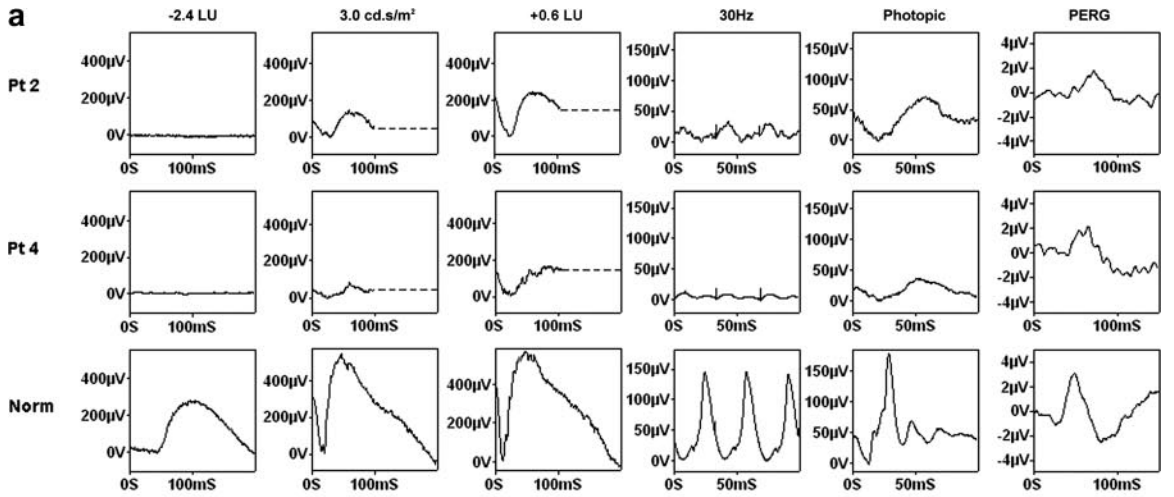

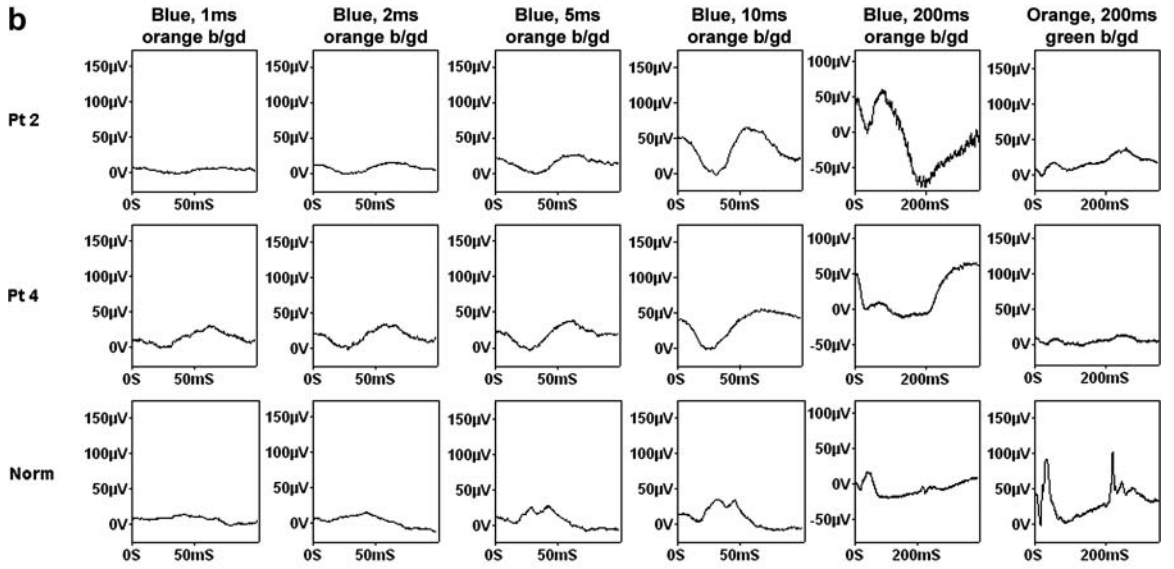

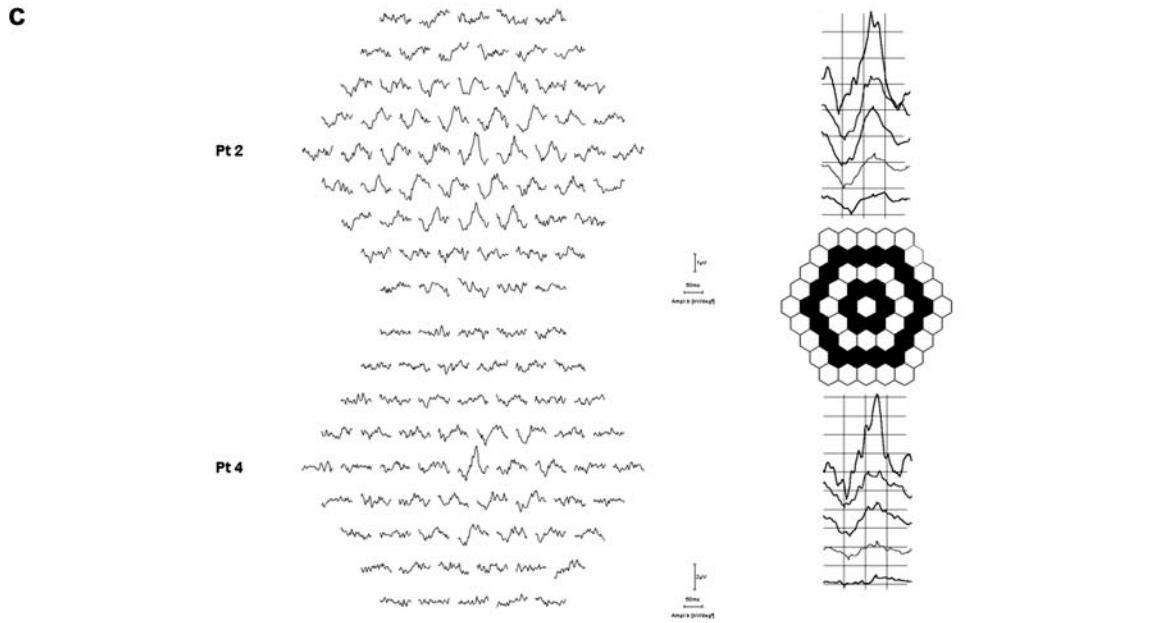

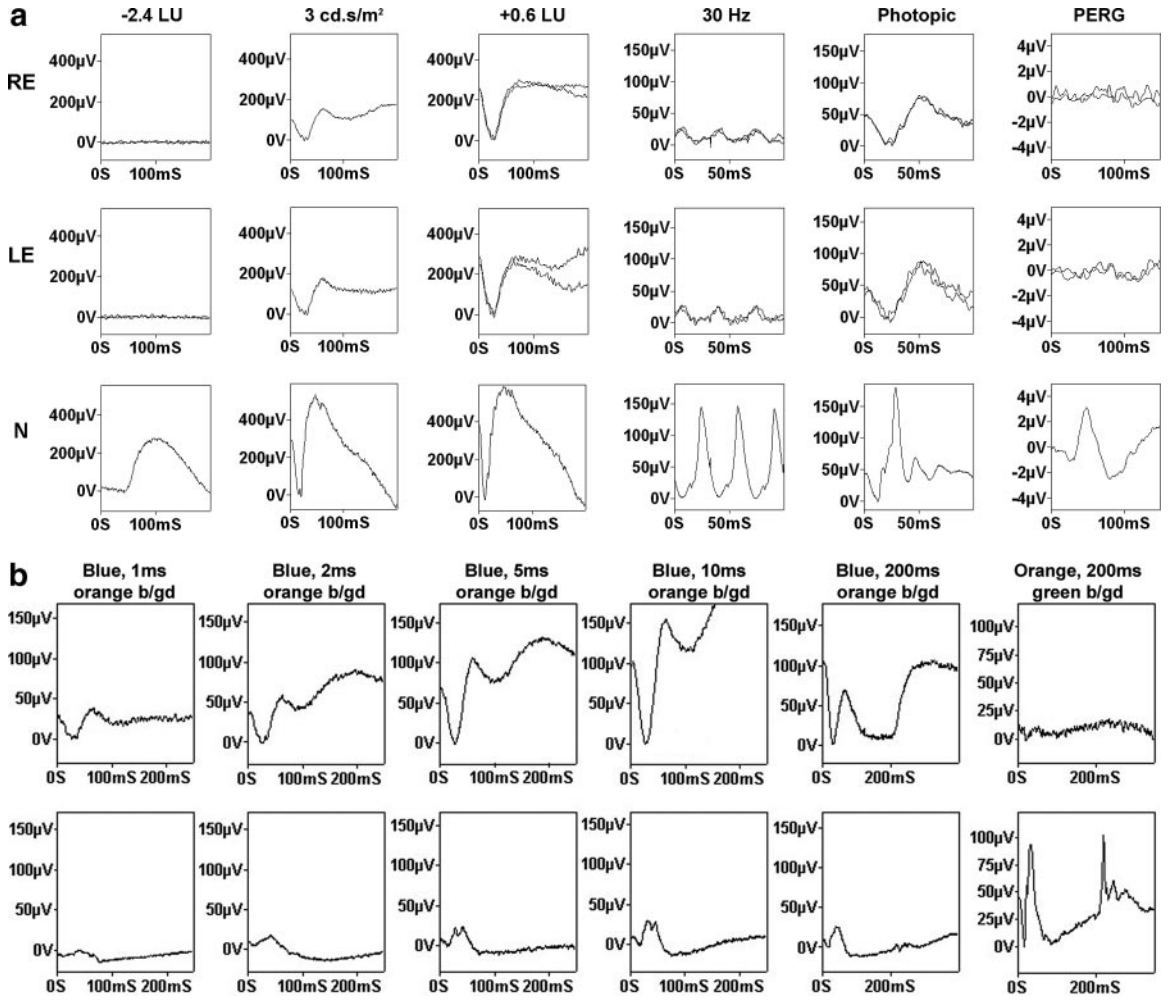

FIGURE 4. (**a**) ISCEV ERGs, PERGs, and (**b**) S-cone-specific ERGs and ON/OFF ERGs of patient 14, a 25-year-old man with nyctalopia and visual acuity of 6/18 in the right eye and 6/36 in the left (Fig 1b). Initial presentation was with loss of central vision secondary to foveal schisis. ERGs are similar to those in Figure 3. Note the prominent apparent OFF response to long-duration S-cone-specific stimulation. PERGs are undetectable in keeping with severe macular dysfunction. Color contrast sensitivity showed tritan sparing.

dus findings in ESCS. Furthermore, this nummular pigmentary retinopathy is not specific to ESCS, since similar fundus abnormalities have been reported in Bardet-Biedl syndrome,[36] in RP with preserved para-arteriolar RPE (RP12, associated with mutation in *CRB1*),[37–39] and in non-syndromic RP.[7,40] The association of these nummular pigmentary deposits with white-yellow dots at the level of the RPE along the vascular arcades, focal hyperpigmentation within the arcades, and foveal or peripheral schisis is more suggestive of ESCS. Small hyperpigmented areas and white dots were also seen within the vascular arcades in some patients. These dots were associated with a focal increase in AF. These abnormalities may be related to those in the *rd7* mouse, which harbors a homozygous deletion in *NR2E3* and displays retinal white dots early in the disease process that histologically correspond to rosettes of dysplastic photoreceptors and which disappear with age.[11,12]

All subjects included in the study had typical electrophysiological findings of short-wavelength–sensitive pathway predominance, with severely reduced L- and M-cone function and no detectable rod ERGs.[3,4] In addition, the ERG findings in all patients where they were detectable, were pathognomonic of ESCS: the rod-specific ERG was undetectable; the ERG to a

FIGURE 3. (**a**) ISCEV standard ERGs and PERG, from patient 2 (Fig. 1c) with 20/20 visual acuity and patient 4, a 19-year-old female with 20/30 vision in both eyes (Fig. 1a). Normal findings appear in the lower row. *Dotted lines* replace blink artifact. The findings from both patients (right eye shown) are diagnostic of enhanced S-cone syndrome. There is no detectable rod-specific response; the standard and brighter flash ERGs are simplified and markedly delayed; the ERGs to a standard single flash have a similar waveform under photopic and scotopic conditions; and the 30 Hz flicker ERG is both delayed and of lower amplitude than the single flash photopic ERG a-wave. The PERG is of borderline amplitude and markedly delayed in patient 2, moderately delayed in patient 4. (**b**) S-cone specific and ON-/OFF-ERGs, from both patients show higher amplitudes, simplified waveforms, and marked peak time delay compared to normal. Note that going from a 10-ms stimulus to a 200-ms stimulus in patient 2 there is minimal change and no evidence of OFF response activity, but in patient 4 the b-wave drops by 80% and there appears to be an OFF response. The drop in b-wave amplitude suggests that OFF activity may contribute to the b-wave evoked by the 10-ms stimulus. All blue stimuli were superimposed upon a high-intensity orange background. (**c**) Multifocal ERGs from patients 2 and 4 show preservation of central responses, better in patient 2, which are delayed and of simplified waveform. The ring analysis (see schematic) goes from the center to the periphery, with the central response being uppermost. Calibration for mfERG: 50 ms; 1 μV for upper trace array, 2 μV for lower trace array.

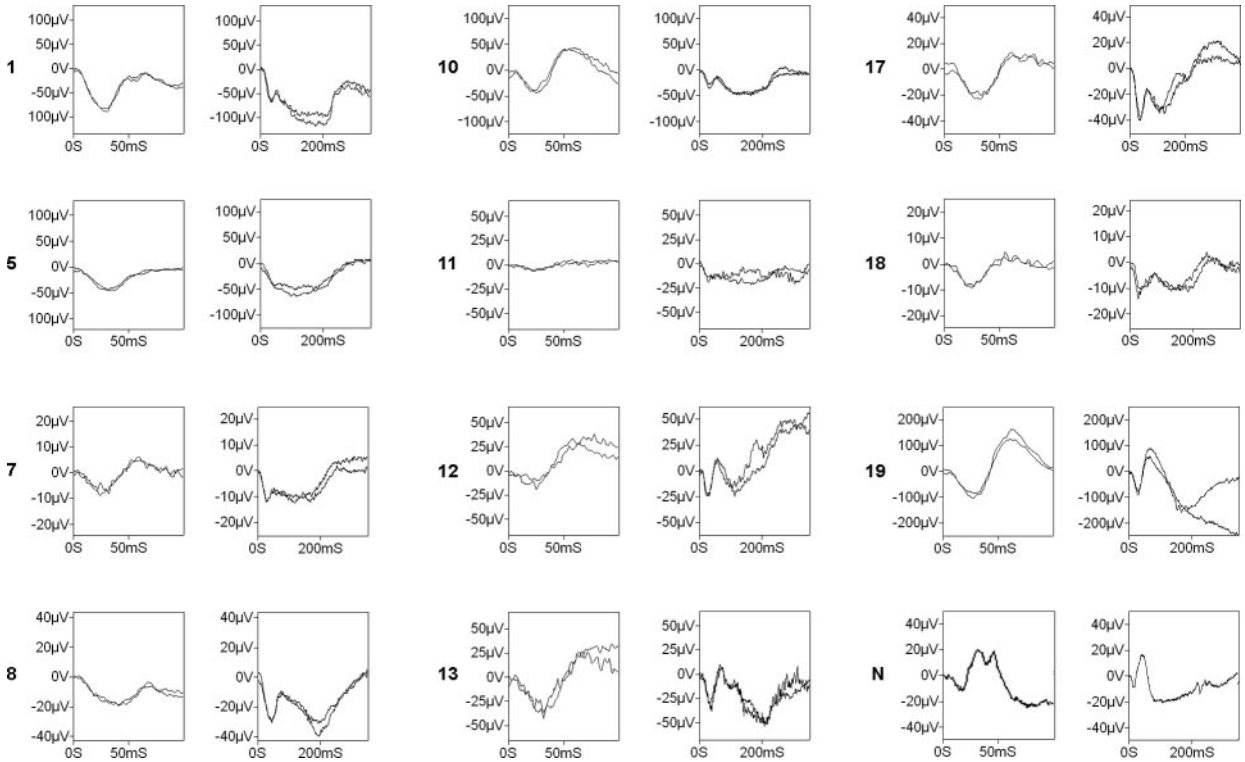

FIGURE 5. ERGs in response to short-wavelength stimulation. Data are shown for all patients for whom results are available. For each patient, the traces are shown for 10-ms (*left*) and 200-ms (*right*) stimulation. N, normal. In all patients, the short-duration stimulus evoked a simplified and highly delayed waveform relative to normal, characteristic of the disorder. Note the absence of the earlier (~30 ms) component in the normal eye that relates to L/M-cone function.[22] Some patients (1, 5, 7, 10, 17, and 18) showed a clear reduction in b-wave amplitude after the increase in stimulus duration from 10 to 200 ms, with no associated change in a-wave amplitude, suggesting that OFF activity may be involved in b-wave for the 10-ms stimulus. Other patients did not show that phenomenon (8, 12, 13, and 19). The data are not clear in the low-amplitude responses of patient 11. Those with b-wave reduction show possible OFF activity.

standard flash was simplified and delayed, with a similar waveform under photopic and scotopic conditions; and, also of importance, the 30-Hz flicker was delayed and of lower amplitude than the single-flash photopic ERG a-wave, ESCS being the only disorder of which these authors are aware in which that is the case. Further, abnormally large, delayed, simplified waveform S-cone ERG responses (relative to the size of the conventional ERGs) were present in all patients tested, confirming the sensitivity to short-wavelength stimulation characteristic of the disorder, but not necessary in making the diagnosis. Responses

TABLE 4. *NR2E3* Disease-Causing Mutations

Affected Individuals	*NR2E3* Mutation	Predicted Change
1	**Hm splice acceptor intron 8 (G→A)(IVS8-1G>A)**	**Aberrant splicing**
2	Not tested	
3	**Hm 145G→A**	**V49M**
4	Ht splice acceptor intron 1 (A→C)(IVS1-2A>C)	Aberrant splicing
	Ht 932G→A	R311Q
5	Not tested	
6	Ht splice acceptor intron 1 (A→C) (IVS1-2A>C)	Aberrant splicing
7	Ht splice acceptor intron 1 (A→C) (IVS1-2A>C)	Aberrant splicing
	Ht 242A→G	**Y81C**
8	Ht splice acceptor intron 1 (A→C) (IVS1-2A>C)	Aberrant splicing
	Ht 242A→G	**Y81C**
9	Hm 500C→T	R104W
10	Hm 500C→T	R104W
11	Hm splice acceptor intron 1 (A→C) (IVS1-2A>C)	Aberrant splicing
12	Not tested	
13	**Hm splice acceptor intron 1 (C→G)(IVS1-3C>G)**	**Aberrant splicing**
14	No mutation found	
15[2]	Hm frameshift mutation T161fs (481delA)	Protein truncation
16	Hm frameshift mutation T161fs (481delA)	Protein truncation
17, 18, 19	Not tested	

Mutations in **bold** represent novel alterations. Ht, heterozygous; Hm, homozygous.

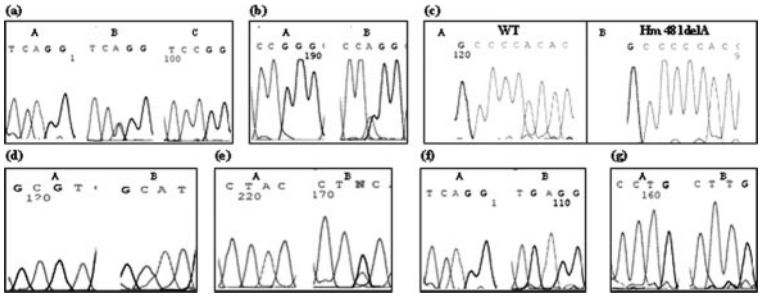

FIGURE 6. Electropherograms showing mutations in *NR2E3*. (**a**) *NR2E3* splice acceptor intron 1 mutation (IVS1-2A>C): A, wild-type (Wt) Exon 2; B, Ht A→C splice variant; C, Hm A→C splice variant; (**b**) *NR2E3* R311Q mutation; A-Wt Exon 6; B, Ht R311Q; (**c**) *NR2E3* 481delA mutation; A, Wt Exon 4; B, Hm 481delA (brothers); (**d**) *NR2E3* V49M mutation; A, Wt Exon 2; B, Hm V49M; (**e**) *NR2E3* Y81C mutation; A, Wt Exon 2; B, Ht Y81C; (**f**) *NR2E3* splice acceptor intron 1 mutation (IVS1-3C>G): A, Wt Exon 2; B, Hm C→G splice variant; (**g**) *NR2E3* splice acceptor intron 8 mutation (IVS8-1G>A): A, Wt Exon 9; B, Hm G→A (C→T) splice variant.

to high-intensity, long-duration orange stimulus on a green background were severely subnormal in all patients, in keeping with reduced L/M-cone function. The amplitude of the ERG was variable across patients with a tendency toward lower amplitudes in older patients, some of whom had profound global ERG reduction, but in whom the findings were otherwise qualitatively similar. The absence of an EOG light increase can be related to the absence of rod photoreceptors.

The spatial extent and degree of mfERG preservation varied between patients and paralleled the PERG findings. Patients with normal amplitude central responses and paracentral sparing had higher amplitude PERG P50 components (e.g., cases 2 and 4), in keeping with a lesser degree of macular dysfunction, than those in which only the central mfERG showed sparing or relative sparing (e.g., case 5). Correlation between mfERGs and PERGs have been reported in cases of RP[33,41] in which central photopic function is preserved in the presence of encroaching paracentral dysfunction. The current findings extend those previously described in a single case of ESCS in which mfERGs revealed greater peripheral than central abnormalities.[42] The PERG data are noteworthy; the profound delay present in some patients is an unusual and novel observation.

The responses to long-duration stimulation using a blue flash with an orange background are of particular interest. The reduction in b-wave amplitude in most of the patients when stimulus duration was increased from 10 to 200 ms, accompanied by an unchanged a-wave, suggests that OFF activity may contribute to the short-duration blue-flash b-wave. It is also those patients in whom there is the presence of possible offset-related responses at the cessation of the 200-ms stimulus. Equally, those patients in whom there was no apparent OFF activity showed no reduction in b-wave amplitude when stimulus duration was increased. Similar findings have been reported,[26] and the current data confirm and extend those observations. In normal retina, L- and M-cone transmission at a postreceptoral level takes place through both ON (depolarizing)- and OFF (hyperpolarizing)-bipolar cells. Foveal S-cones may contact S-cone OFF midget bipolar cells[43] but rods and peripheral S-cones are thought to connect only to ON-bipolar cells.[44] The existence of possible OFF-related ERG activity in most patients, albeit atypical, may suggest that the short-wavelength–sensitive cone system in ESCS transmits information in a manner more usually associated with L- and M-cones than with the classic S-cone pathway. This may reflect a default pathway from L/M-cone differentiation; may be the result of atypical second-order neuronal networks, such that S-cones synapse with both ON- and OFF-bipolar cells; or may be sec-

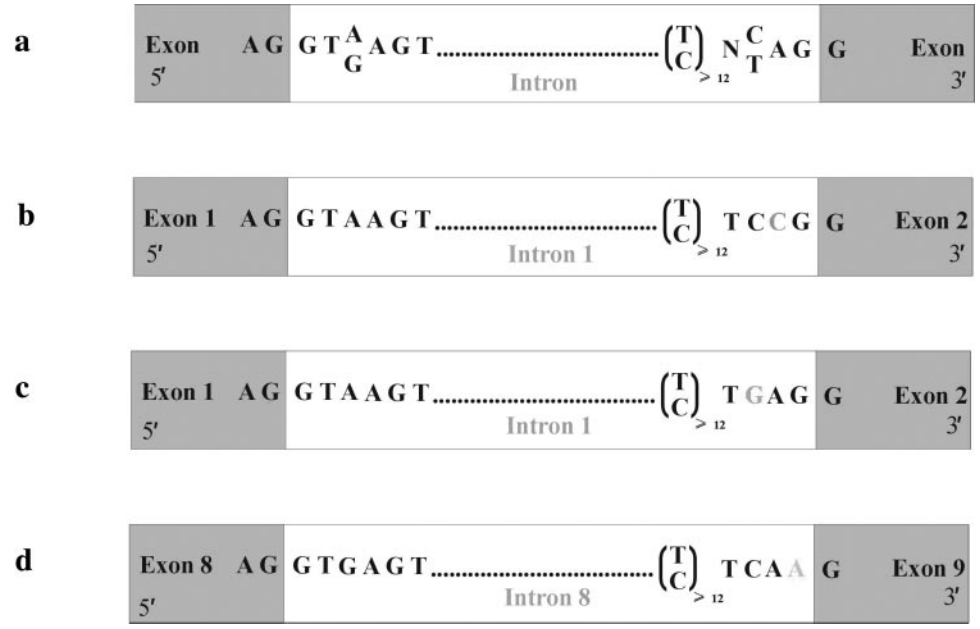

FIGURE 7. Consensus sequences for 5′ and 3′ splice sites in nuclear protein-coding genes and location of splice site mutations (*gray*) identified in *NR2E3*. (**a**) Consensus sequences for 5′ and 3′ splice sites. *Shaded*: exons; *unshaded*: intervening intronic sequence. (**b**) A/C splice acceptor mutation in intron 1 identified previously and in this study. (**c**) Novel C/G splice acceptor mutation in intron 1. (**d**) Novel G/A splice acceptor mutation in intron 8.

ondary to replacement of L- and M-cone opsins by short-wavelength–sensitive opsin.

The absence of rods in ESCS is now better understood. NR2E3 has exclusively been localized to the nuclei of rods in mature human, mouse, and zebrafish retina and is also detectable during retinal development.[15,16] NR2E3 has recently been shown to have a transcriptional repressive effect on cone-specific genes in rod photoreceptors.[16] Functional inactivation of NR2E3 could result in the failure of rods and photoreceptors to develop that adopt an S-cone phenotype, leading to the increased number of S-cones seen in ESCS at the expense of rod photoreceptors.[16] The cause of the slow retinal degeneration observed in ESCS is more difficult to explain, but may include the inability of cone cells to survive in the absence of rod photoreceptors.[45,46] Currently, less is understood about cone cell differentiation. How *NR2E3* mutations result predominantly in an increased S-cone population is not established.

Mutations in *NR2E3* were identified in 12 of the 13 patients who consented to give blood. Eight sequence variants in the coding region were found that most likely represent disease-causing mutations. Four of these are novel: two splice acceptor mutations, at introns 1 and 8, respectively, and two missense mutations, Val49Met and Tyr81Cys. The first novel splice site mutation (C→G nucleotide change) is located at the same intron 1 splice acceptor site previously identified as harboring one of the most common sequence variations in ESCS, that being an A→C change present in ~35% to 50% of subjects.[6,8] In the present study this A→C change was similarly frequently identified in ~45% of subjects screened. The second novel splice acceptor mutation is at intron 8 (G→A change). A region not previously identified as harboring potentially disease-causing sequence variants. The splice acceptor introns 1 and 8 mutations would both be predicted to cause aberrant splicing, resulting in either a truncated nonfunctional protein, or one of significantly reduced transcriptional activity since exons 2 and 9 encode residues involved in DNA-binding and ligand-binding, respectively. The splice acceptor intron 1 mutation would also result in a frameshift and premature stop codon in exon 3, if exon 2 was deleted, with the resultant transcript most likely undergoing nonsense-mediated mRNA decay. The subject homozygous for the splice acceptor mutation in intron 8 has a mild phenotype, which may reflect her young age or may indicate that this splice site mutation has a less severe effect on receptor function, being located at the last coding exon, and thus predicted to affect only the terminal portion of the ligand-binding domain. The novel mutations V49M and Y81C are both located in the highly conserved DNA-binding domain of NR2E3. The subject homozygous for the V49M mutation has milder disease than other members of the panel. This mutation is located at the start of the proposed DNA-binding domain, whereas Y81C is in the central region of this domain. The individuals with the Y81C mutation were compound heterozygotes, thereby precluding a direct comparison; however, they were more severely affected, suggesting that the V49M may have a less adverse effect on DNA-binding. T161fs (481delA) will generate a premature stop codon at position 178 and is therefore the only nonsense mutation described in ESCS to date, having been identified in the homozygous state in this study and previously as a heterozygous change.[8] This 1-bp deletion will most likely undergo nonsense-mediated mRNA decay. However, if this allele were translated, the truncated protein would lack the ligand-binding domain and would be nonfunctional. Therefore, whatever the precise molecular outcome of this mutation, it is likely that subjects homozygous for it would have a more severe phenotype than would heterozygous individuals. The previous report does not provide sufficient clinical data to enable such a comparison, although the two brothers in the present panel with this homozygous mutation have a relatively severe phenotype at a young age compared with other subjects.

No disease-causing sequence variants were identified in one patient with typical clinical and electrophysiological signs of ESCS, and only a heterozygous mutation was detected in another subject. It may be that the mutations in these cases are intronic, in the promoter, or present in as yet unidentified exons. In addition, heterozygous deletions may also have been missed by direct sequencing; Southern blot analysis or quantitative PCR may be useful techniques in identifying individuals with such deletions. It also cannot be absolutely excluded that there is further genetic heterogeneity to be identified, with candidate genes including *NRL* and *THRB1*.[6,47,48] Although the four novel mutations identified in this study and other previously described mutations[6–8] appear likely to be disease-causing on the basis of either aberrant splicing or location at highly conserved domains critical to protein function, only functional studies assessing the effects of these sequence variants on NR2E3 stability, targeting, and ability to interact effectively and reversibly with either DNA or ligand, can provide definitive supportive evidence of pathogenicity.

In conclusion, patients with ESCS exhibit a variable clinical phenotype associated with various degrees of pigmentary change, foveal schisis, and visual loss. The presence of pathognomonic electrophysiological responses establishes the diagnosis and directs appropriate genetic screening and counseling. Uncertainties remain concerning the nature of the electrophysiological signaling in the retinas of these patients.

References

1. Jacobson SG, Marmor MF, Kemp CM, Knighton RW. SWS (Blue) cone hypersensitivity in a newly identified retinal degeneration. *Invest Ophthalmol Vis Sci*. 1990;31:827–838.
2. Marmor MF, Jacobson SG, Foerster MH, Kellner U, Weleber, RG. Diagnostic clinical findings of a new syndrome with night blindness, maculopathy, and enhanced S cone sensitivity. *Am J Ophthalmol*. 1990;110:124–134.
3. Hood DC, Cideciyan AV, Roman AJ, Jacobson SG. Enhanced S cone syndrome: evidence for an abnormally large number of S cones. *Vision Res*. 1995;35:1473–1481.
4. Greenstein VC, Zaidi Q, Hood DC, Spehar B, Cideciyan AV, Jacobson SG. The enhanced S cone syndrome: an analysis of receptoral and post-receptoral changes. *Vision Res*. 1996;36:3711–3722.
5. Milam AH, Rose L, Cideciyan AV, et al. The nuclear receptor NR2E3 plays a role in human photoreceptor differentiation and degeneration. *Proc Natl Acad Sci*. 2002;99:473–478.
6. Haider NB, Jacobson SG, Cideciyan AV, et al. Mutation of a nuclear receptor gene, NR2E3, causes enhanced S cone syndrome, a disorder of retinal cell fate. *Nat Genet*. 2000;24:127–131.
7. Sharon D, Sandberg MA, Caruso RC, Berson EL, Dryja TP. Shared mutations in NR2E3 in enhanced S-cone syndrome, Goldman-Favre syndrome and many cases of Clumped Pigmentary Retinal Degeneration. *Arch Ophthalmol*. 2003;121:1316–1323.
8. Wright AF, Reddick AC, Schwartz SB, et al. Mutation analysis in *NR2E3* and *NRL* genes in enhanced S cone syndrome. *Hum Mut*. 2004;24:439.
9. Hawes NL, Smith RS, Chang B, Davission M, Heckenlively JR, John SWM. Mouse fundus photography and angiography: a catalogue of normal and mutant phenotypes. *Mol Vis*. 1999;5:22.
10. Akhmedov NB, Piriev NI, Chang B, et al. A deletion in a photoreceptor-specific nuclear receptor mRNA causes retinal degeneration in the *rd7* mouse. *Proc Natl Acad Sci USA*. 2000;97:5551–5556.
11. Haider NB, Naggert JK, Nishina PM. Excess cone cell proliferation due to lack of a functional NR2E3 causes retinal dysplasia and degeneration in rd7/rd7 mice. *Hum Mol Genet*. 2001;10:1619–1626.
12. Yanagi Y, Takezawa S, Kato S. Distinct functions of photoreceptor cell-specific nuclear receptor, thyroid receptor beta2 and CRX in

cone photoreceptor development. *Invest Ophthalmol Vis Sci* 2002;43:3489–3494.
13. Kobayashi M, Takezawa S-I, Hara K, et al. Identification of a photoreceptor cell-specific nuclear receptor. *Proc Natl Acad Sci USA*. 1999;96:4814–4819.
14. Peng G-H, Ahmad O, Ahmad F, Liu J, Chen S. The photoreceptor-specific nuclear receptor Nr2e3 interact with Crx and exerts opposing effects on the transcription of rod versus cone genes. *Hum Mol Genet*. 2005;14:747–764.
15. Bumsted O'Brien KM, Cheng H, Jiang Y, Schulte D, Swaroop A, Hendrickson AE. Expression of photoreceptor-specific nuclear receptor NR2E3 in rod photoreceptor of fetal human retina. *Invest Ophthalmol Vis Sci*. 2004;45:2807–2812.
16. Chen J, Rattner A, Nathans J. The rod photoreceptor-specific nuclear receptor Nr2e3 represses transcription of multiple cone-specific genes. *J Neurosci*. 2005;25:118–129.
17. Chen S, Wang QL, Nie Z, et al. Crx, a novel Otx-like paired-homeodomain protein, binds to and transactivates photoreceptor cell-specific genes. *Neuron*. 1997;19:1017–1030.
18. Szel A, van Veen T, Rohlich P. Retinal cone differentiation. *Nature*. 1994;370:336.
19. Szel A, Juliusson B, Bergstrom A, Wilke K, Ehinger B, van Veen T. Reversed ratio of color-specific cones in rabbit retinal cell transplants. *Brain Res Dev Brain Res*. 1994;81:1–9.
20. Bach M, Hawlina M, Holder GE, et al. Standard for pattern electroretinography. *Doc Ophthalmol*. 2000;101:11–18.
21. Marmor MF, Holder GE, Seeliger MW, Yamamoto S. International Society for Clinical Electrophysiology of Vision: standard for clinical electroretinography (2004 update). *Doc Ophthalmol.* 2004; 108:107–114.
22. Arden GB, Wolf J, Berninger T, Hogg CR, Tzekov R, Holder GE. S-cone ERGs elicited by a simple technique in normals and in tritanopes. *Vision Res*. 1999;39:641–650.
23. Arden GB, Gunduz K, Perry S. Colour vision testing with a computer graphics system. *Clin Vis Sci*. 1988;2:303–320.
24. Holder GE, Votruba M, Carter AC, Bhattacharya SS, Fitzke FW, Moore AT. Electrophysiological findings in Dominant Optic Atrophy (DOA) linking to the OPA1 locus on chromosome 3q 28-qter. *Doc Ophthalmol*. 1999;95:217–228.
25. Jacobson SG, Roman AJ, Roman MI, Gass JD, Parker JA. Relatively enhanced S-cone function in the Goldman-Favre syndrome. *Am J Ophthalmol*. 1991;111:446–453.
26. Roman AJ, Jacobson SG. S cone-driven but not S-cone-type electroretinograms in the enhanced S cone syndrome. *Exp Eye Res*. 1991;53:685–690.
27. Dorey CK, Wu G, Ebenstein D, Garsd A, Weiter JJ. Cell loss in the ageing retina: relationship to lipofuscin accumulation and macular degeneration. *Invest Ophthalmol Vis Sci*. 1989;30:1691–1699.
28. von Rückmann A, Fitzke FW, Bird AC. Fundus autofluorescence in age related macular disease imaged with a scanning laser ophthalmoscope. *Invest Ophthalmol Vis Sci*. 1997;38:478–486.
29. Robson AG, Egan C, Holder GE, Bird AC, Fitzke FW. Comparing rod and cone function with fundus autofluorescence images in retinitis pigmentosa. *Adv Exp Med Biol*. 2003;533:41–47.
30. Robson AG, El-Amir A, Bailey C, et al. Pattern ERG correlates of abnormal fundus autofluorescence in patients with retinitis pigmentosa and normal visual acuity. *Invest Ophthalmol Vis Sci*. 2003;44:3544–3550.
31. Robson AG, Egan CA, Luong VA, Bird AC, Holder GE, Fitzke FW. Comparison of fundus autofluorescence with photopic and scotopic fine-matrix mapping in patients with retinitis pigmentosa and normal visual acuity. *Invest Ophthalmol Vis Sci*. 2004;45: 4119–4125.
32. Michaelides M, Holder GE, Hunt DM, Fitzke FW, Bird AC, Moore AT. A detailed study of the phenotype of an autosomal dominant cone-rod dystrophy (CORD7) associated with mutation in the gene for RIM1. *Br J Ophthalmol*. 2005;89:198–206.
33. Popovic P, Jarc-Vidmar M, Hawlina M. Abnormal fundus autofluorescence in relation to retinal function in patients with retinitis pigmentosa. *Graefes Arch Clin Exp Ophthalmol*. 2005;243:1018–1027.
34. Robson AG, Michaelides M, Luong V, et al. Functional correlates of fundus autofluorescence abnormalities in patients with RPGR or RIMS1 mutations causing cone or cone rod dystrophy. *Br J Ophthalmol*. 2008;92:95–102. Epub 2007 Oct 25.
35. Robson AG, Michaelides M, Saihan Z, et al. Functional characteristics of patients with retinal dystrophy that manifest abnormal parafoveal annuli of high density fundus autofluorescence; a review and update. *Doc Ophthalmol*. 2008;116:79–89. Epub 2007 Nov 6.
36. Franceschetti A, François J, Babel J. *Chorioretinal Heredodegenerations*. Springfield, IL: Charles C. Thomas Publisher; 1974.
37. Heckenlively JR. Preserved para-arteriole retinal pigment epithelium (PPRPE) in retinitis pigmentosa. *Br J Ophthalmol*. 1982;66: 26–30.
38. van den Born LI, van Soest S, van Schooneveld MJ, Riemslag FC, de Jong PT, BleekerWagemakers EM. Autosomal recessive retinitis pigmentosa with preserved para-arteriolar retinal pigment epithelium. *Am J Ophthalmol*. 1994;118:430–439.
39. den Hollander AI, ten Brink JB, de Kol YJ, et al. Mutations in a human homologue of Drosophila crumbs cause retinitis pigmentosa (RP12). *Nat Genet*. 1999;23:217–221.
40. To KW, Adamian M, Jakobiec FA, Berson EL. Clinical and histopathological findings in clumped pigmentary retinal degeneration. *Arch Ophthalmol*. 1996;114:950–955.
41. Robson AG, Saihan Z, Jenkins SA, et al. Functional characterisation and serial imaging of abnormal fundus autofluorescence in patients with retinitis pigmentosa and normal visual acuity. *Br J Ophthalmol*. 2006;90:472–479.
42. Marmor MF, Tan F, Sutter EE, Bearse MA Jr. Topography of cone electrophysiology in the enhanced S cone syndrome. *Invest Ophthalmol Vis Sci*. 1999;40:1866–1873.
43. Klug K, Herr S, Ngo IT, Sterling P, Schein S. Macaque retina contains a S-cone OFF midget pathway. *J Neurosci*. 2003;23:9881–9887.
44. Kolb H, Goede P, Roberts S, McDermott R, Gouras P. Uniqueness of the S-cone pedicle in the human retina and consequences for color processing. *J Comp Neurol*. 1997;386:443–460.
45. Hicks D, Sahel J. The implication of rod-dependent cone survival for basic and clinical research. *Invest Ophthalmol Vis Sci*. 1999; 40:3071–3074.
46. Léveillard T, Mohand-Saïd S, Lorentz O, et al. Identification and characterization of rod-derived cone viability factor. *Nat Genet.* 2004;36: 755–759.
47. Mears AJ, Kondo M, Swain PK, et al. NRL is required for rod photoreceptor development. *Nat Genet*. 2001;29:447–452.
48. Ng L, Hurley JB, Dierks B, et al. A thyroid hormone receptor that is required for the development of green cone photoreceptors. *Nat Genet*. 2001;27:94–98.